

FRACTURE INITIATION AND PROPAGATION BEHAVIORS OF THINLY INTERBEDDED TIGHT SANDSTONE RESERVOIRS BY VARIOUS HYDRAULIC FRACTURING METHODS

by

Yong CHEN^a, Zhihao XIA^{a,b,*}, Tian LAN^{a,b},

^aCNOOC Energy Development Co., Ltd

^bNational Key Laboratory of Petroleum Resources and Engineering, China University of Petroleum, Beijing, 102249, China

This paper proposed three new fracturing methods, slick water with an integrated variable viscosity fracturing, supercritical CO₂ shock fracturing and pulse hydraulic fracturing. To verify the efficacy of the new methods, we conducted laboratory true-triaxial fracturing experiments by using outcrops collected from the Lower Shihezi formation, Ordos Basin. The results indicate that supercritical CO₂ shock fracturing is observed to have the lowest breakdown pressure compared with other methods.

Key words: *Thinly interbedded reservoir, thermal stress, fatigue damage, CO₂ fracturing, pulse hydraulic fracturing, slick water fracturing*

Introduction

Tight gas reservoirs in the Ordos Basin contribute a considerable proportion in China hydrocarbon resource and large reserves remain to be developed substantially. Efficiently exploitation such resources are of great significance in meeting the ever-increasing energy demands and ensuring national energy security. Hydraulic fracturing is a common method to increase gas production from multi-layered formations. However, high breakdown pressure, single main fractures and environmental burdens have long been the problems facing by the conventional hydraulic fracturing techniques. As a result, both industry and academics have been struggling to find novel reservoir stimulation alternatives. Zimmermann et al, Yu et al found that pulse hydraulic fracturing injection can reduce the breakdown pressure of rocks and create more complicated fractures compared to conventional hydraulic fracturing [1]. Zhu et al found that Supercritical CO₂ (SC-CO₂) might be a potential substitute for water-based fracturing fluid widely used in the present hydraulic fracturing of reservoirs as SC-CO₂ fracturing generates more fractures with greater bifurcation and higher tortuosity [2]. Moreover, slick water fracturing with an integrated variable viscosity has been tested in field site due to its ability to generate a major fracture combined with numerous branches [3]. However, the above studies focused on a single fracturing method and the specimens used are mostly shale and granite, it is important to note that thinly inter-bedded tight sandstone possesses numerous natural bedding planes leading to different modes of fracture initiation and propagation compared with

* Corresponding author, e-mail: 18810597102@163.com

shale and granite. Comparative studies on fracture initiation and propagation behaviors of thinly inter-bedded tight sandstone under the true triaxial stress conditions by different fracturing methods are insufficient.

In this study, outcrops collected from the Lower Shihezi formation, Ordos Basin were selected and hydraulic fracturing tests of thinly inter-bedded tight sandstone under different test schemes (slick water with an integrated variable viscosity fracturing, supercritical CO₂ shock fracturing and pulse hydraulic fracturing) were carried out to simulate breakdown pressure and fracture propagation behavior on-site construction.

Experimental apparatus and scheme

Experimental specimen

The rock specimens used in this study were collected from Ordos Basin in Lower Shihezi formation. As shown in Fig.1, it can be found that the core specimen is thinly interbedded sandstone-mudstone. The specimens were cut into the size of 100 mm×100 mm×100 mm and prefabricated a borehole of Φ16 mm diameter and 60 mm length in the center of the cubic specimens relatively perpendicular to the beddings by an impact-resistant bench drill. The size of the wellbore was Φ14 mm diameter and 40 mm length and fixed in the borehole using epoxy-resinadhesive. Furthermore, a 3D handheld profile meter was employed to accurately capture the complexity of the actual fractures within the rock specimen.

Rock mechanics tests revealed an average porosity of 11.60% and an average permeability of 0.24 mD, indicating a formation with low porosity and low permeability. The Young's modulus and the Poisson's ratio exhibited a value of 30.13 MPa and 0.26 under the condition close to the confining pressure of the reservoir (30 MPa).

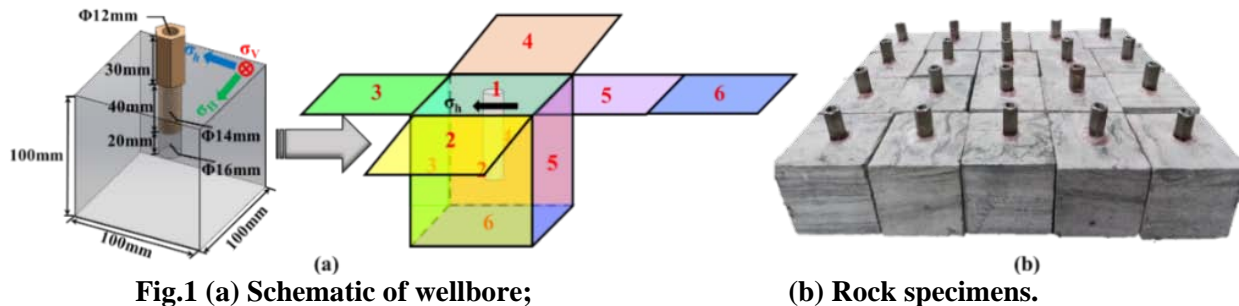


Fig.1 (a) Schematic of wellbore;

(b) Rock specimens.

Experimental apparatus and scheme

The true-triaxial fracturing equipment was depicted in Fig.2, which consists of a supercritical CO₂ injection system, a liquid pulse pump injection system, a water injection system, a true triaxial-loading unit and a data acquisition system. The detailed descriptions of the systems can be seen in our previous work [4].

The main objective of this paper is to study the fracture patterns and breakdown pressures associated with different fracturing methods. As shown in Table1, 9 groups of experiments were conducted in this study under different fracturing methods with the initial true-triaxial stresses set as $\sigma_h=6$ MPa, $\sigma_H=8$ MPa, and $\sigma_v=10$ MPa, which was determined by similarity criterion based on field data. During the slick water with an integrated variable viscosity fracturing test, water and diethyl silicone oil with a viscosity of 50 mPa·s were injected in different steps, at a constant injection rate of 30 mL/min, until a peak pressure was reached, and the measured pressure is the breakdown pressure of the specimen. For the supercritical CO₂ shock fracturing and pulse hydraulic fracturing tests, supercritical CO₂ and water were injected into the wellbore respectively under different shock

pressures and peak pressures to investigate their effects on fracture patterns. Besides, colored-water and fluorescent tracer were added to visualize the fractures after the fracturing tests to observe the fracture patterns inside the rock specimens.

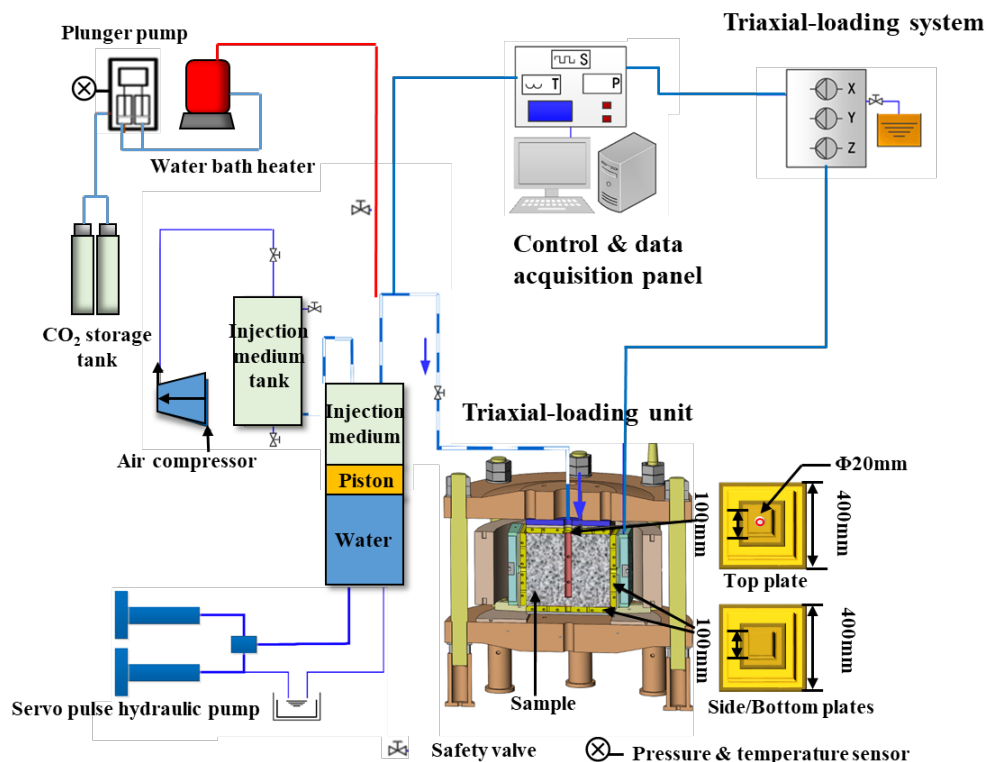


Fig.2 True-triaxial fracturing equipment.

Table.1Matrix of fracturing experiments performed under triaxial stresses.

Type	Rock specimen number	$\sigma_v/\sigma_H/\sigma_h$ (MPa)	Injection rate/pressure
Conventional water-based hydraulic fracturing	B-1	10/8/6	30 mL/min
	B-2	10/8/6	6 MPa
Pulse hydraulic fracturing	B-3	10/8/6	8 MPa
	B-4	10/8/6	10 MPa
Supercritical CO ₂ shock fracturing	B-5	10/8/6	12 MPa
	B-6	10/8/6	16 MPa
	B-7	10/8/6	20 MPa
slick water with an integrated variable viscosity fracturing	B-8	10/8/6	30 mL/min (water + dimethyl silicone oil)
	B-9	10/8/6	30 mL/min (dimethyl silicone oil +water)

Experimental results and discuss

Comparison of breakdown pressure under different fracturing methods

The breakdown pressures achieved by different fracturing methods, including conventional water-based hydraulic fracturing, pulse hydraulic fracturing, supercritical CO₂ shock fracturing, and slick water with an integrated variable viscosity fracturing were compared in Fig.3. It is evident from

the graph that supercritical CO₂ shock fracturing exhibited the lowest average breakdown pressure among the compared methods. This can be attributed to the significant reduction in rock breakdown pressure resulting from the combined effect of thermal stress, shock waves, and fluid pressure during supercritical CO₂ fracturing. This method consequently requires relatively low pressure within the fractures to induce fracture extension[5]. In addition, pulse hydraulic fracturing, owing to its pulse shock characteristics, also substantially decreased the rock breakdown pressure. The high fluid pressures generated during the propagation of pulse fluid pressure surpass their inherent energy source, consequently causing reciprocal impact damage to the specimen and reducing the fracture pressure. Moreover, the breakdown pressure in specimen B-8 was 5.3 MPa lower than that in specimen B-9 due to the higher fluid viscosity associated with a greater flow resistance during the hydraulic fracturing process. This increase in flow resistance leads to a higher consumption of energy required to drive the fluid flow within the fracture.

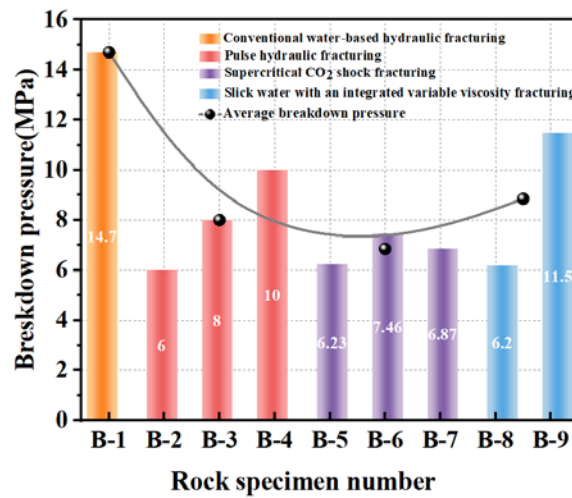


Fig.3 Statistical values of the breakdown pressure by different hydraulic fracturing methods.

Comparison of fracture pattern under different fracturing methods

Fracture morphologies of different fracturing methods are shown in Fig.4. Fig. 4a (Specimen B-1) shows the fracture initiation and propagation behaviors of the conventional water-based-hydraulic-fracturing experiments. It can be found that the fracture initiated in the sand layer and slipped along the adjacent bedding plane resulting in a simply single main fracture.

Fig. 4b, 4c and 4d (Specimens B-2, B-3 and B-4) depict fracture initiation and propagation behaviors observed during pulse hydraulic fracturing experiments. Unlike conventional water-based hydraulic fracturing experiments, these specimens displayed a unique phenomenon where fractures gradually became flexural and inclined while crossing bedding planes. At pulse hydraulic peak pressures of 6 MPa and 8 MPa, a single main fracture was formed across the bedding planes with a certain angle. However, at a pulse hydraulic peak pressure of 10 MPa, the boundary between the sand and mud layers was activated and complex fracture networks were generated, characterized by a “main fracture + activated bedding plane”. The phenomenon can be attributed to the “Water Hammer Effect” in which the peak pressure generates an instantaneous impact force that surpasses the hydraulic energy of the fluid within the specimen. Consequently, impact damage facilitated by the effect can connect micro-cracks and benefit in fracture propagation [6].

Fig. 4e, 4f and 4g (Specimens B-5, B-6 and B-7) depict the fracture initiation and propagation behaviors observed during supercritical CO₂ shock fracturing experiments. When the shock pressures were 12 MPa and 16 MPa, two activated bedding plane were generated inside rocks. When the shock

pressure was 20 MPa, the fractures propagated along the bedding surface firstly, then penetrating through the bedding plane, and eventually halted by the upper and lower surfaces of the rock specimen. This process resulted in the formation of multiple fractures that were interconnected, consisting of a main fracture and branch fractures. It can be concluded that the fracture patterns displayed branching characteristic as the shock pressure increased. On the whole, supercritical CO₂ shock fracturing can increase the complexity and conductivity of the fractures compared to conventional water-based hydraulic fracturing due to the combined effect of thermal stress, shock waves and fluid pressure [7].

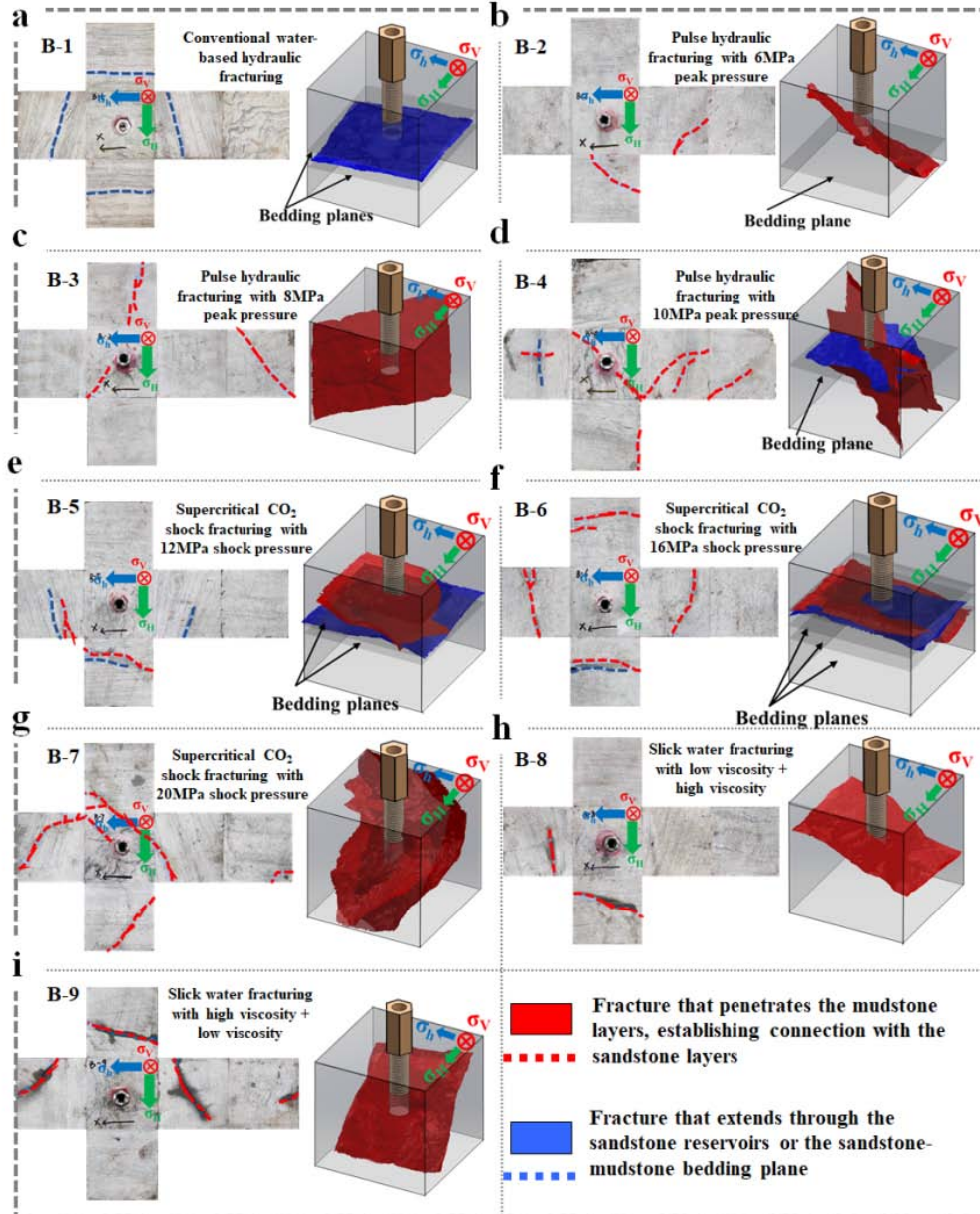


Fig.4 Fracture patterns of different fracturing method

Fig. 4h and 4i (Specimens B-8 and B-9) depict the fracture initiation and propagation behaviors observed during slick water with an integrated variable viscosity fracturing. Compared to conventional water-based hydraulic fracturing, the specimens in this study exhibited fracture penetrated both the sand and mud layers. Additionally, the fracturing performance of the first injecting high viscosity slick water followed by low viscosity slick water was found to be superior to the first injecting low viscosity slick water followed by high viscosity slick water and conventional water-based hydraulic fracturing. This is attributed to the application of high viscosity slick water during the initial stage to

create main fractures, and the subsequent use of low-to-medium viscosity slick water to activate natural fractures and carry proppants during the proppant-laden stage [8]. As a result, a major fracture combined with numerous branches was generated.

Conclusions

In this study, the true-triaxial laboratory experiments of conventional water-based hydraulic fracturing, pulse hydraulic fracturing, supercritical CO₂ shock fracturing, and slick water with an integrated variable viscosity fracturing were conducted to explore the fracture initiation and propagation behaviors under different fracturing methods.

Acknowledgments

This work is supported by the National Natural Science Foundation of China (National R&D Program for Major Research Instruments, 51827804)

References

- [1] Li, Q., *et al.*, the Effect of Pulse Frequency on the Fracture Extension During Hydraulic Fracturing, *Journal of Natural Gas Science and Engineering*, 21(2014), 11, pp. 296-303
- [2] Cai, C., *et al.*, Fracture Propagation and Induced Strain Response During Supercritical CO₂ Jet Fracturing, *Petroleum Science*, 19.(2022), 4, pp. 1682-1699
- [3] Lu, B., *et al.*, Status and Tendency of Engineering Technology in Shale Gas Development Within Sinopec, *22nd World Petroleum Congress*, 2017, 7, Article IDWPC-22-0608
- [4] Lv, Y., *et al.*, An Experimental Investigation on Influence of Hydraulic Pulse on Hydraulic Fracture, *52nd U.S. Rock Mechanics/Geomechanics Symposium*, 2018, 6, Article IDARMA-2018-957
- [5] Cong, R., *et al.*, Supercritical CO₂ Shock Fracturing on Coal: Experimental Investigation on Fracture Morphology and Pressure Characteristics, *56th U.S. Rock Mechanics/Geomechanics Symposium*, 2022, 6, Article IDARMA-2022-0182
- [6] He, P., *et al.*, Experimental Study on Fracture Propagation and Induced Earthquake Reduction by Pulse Hydraulic Fracturing in Shale Reservoirs, *Gas Science and Engineering*, 110(2023), 6, Article ID204908
- [7] Zou, Y., *et al.*, Experimental Study on the Growth Behavior of Supercritical CO₂-Induced Fractures in A Layered Tight Sandstone Formation, *Journal of Natural Gas Science and Engineering*, 49 (2018), 6, pp. 145-156
- [8] Hou, B., *et al.*, Analysis of Hydraulic Fracture Initiation and Propagation in Deep Shale Formation with High Horizontal Stress Difference, *Journal of Petroleum Science and Engineering*, 170 (2018), 11, pp. 231-243

Paper submitted: July 24, 2023

Paper revised: August 25, 2023

Paper accepted: November 11, 2023